GEOPHYSICAL RESEARCH LETTERS, VOL. 38, L14703, doi:10.1029/2011GL047995, 2011

Reanalysis suggests long-term upward trends in European storminess since 1871

M. G. Donat,[1,2] D. Renggli,[2,3] S. Wild,[2] L. V. Alexander,[1] G. C. Leckebusch,[2,4] and U. Ulbrich[2]

Received 2 May 2011; revised 10 June 2011; accepted 11 June 2011; published 26 July 2011.

[1] Regional trends of wind storm occurrence in Europe are investigated using the 20th Century Reanalysis (20CR). While based on surface observations only, this dataset produces storm events in good agreement with the traditional ERA40 and NCEP reanalyses. Time series display decadal-scale variability in the occurrence of wind storms since 1871, including a period of enhanced storm activity during the early 20th century. Still, significant upward trends are found in central, northern and western Europe, related to unprecedented high values of the storminess measures towards the end of the 20th century, particularly in the North Sea and Baltic Sea regions. **Citation:** Donat, M. G., D. Renggli, S. Wild, L. V. Alexander, G. C. Leckebusch, and U. Ulbrich (2011), Reanalysis suggests long-term upward trends in European storminess since 1871, *Geophys. Res. Lett.*, *38*, L14703, doi:10.1029/2011GL047995.

1. Introduction

[2] Severe wind storms are one of the major natural disasters in Europe, often causing heavy destruction over inland areas, rough sea conditions, and the risk of storm surges in coastal regions. Associated extreme wind speeds typically relate to strong North Atlantic extra-tropical cyclones, traveling eastwards towards the European continent. These storm events affect large areas and often cause high cumulated losses, attracting broad public attention. Climate modeling studies suggest a poleward shift of the mid-latitude storm tracks under future anthropogenic climate conditions [*Meehl et al.*, 2007]. More intense cyclones may form under future climate conditions over the eastern North Atlantic (for a review see *Ulbrich et al.* [2009]), leading to enhanced extreme wind speeds over Europe [*Gastineau and Soden*, 2009; *Donat et al.*, 2011] and more frequent storm occurrence [*Donat et al.*, 2010b]. Note some uncertainties are related to circulation responses in climate projections particularly for the European region [*Woollings*, 2010]. Nevertheless, modeling results suggest that increases in storminess could already be detectable in data from the last century, reflecting related increases in observed greenhouse gas concentrations. Several studies estimating storminess from pressure records, however, could not find evidence for such trends in the recent past. They generally point at large decadal-scale variability, including enhanced occurrence of severe storms in the late 19th to early 20th century and at the end of the 20th century [*Alexandersson et al.*, 1998, 2000; *Bärring and von Storch*, 2004; *Hanna et al.*, 2008; *Wang et al.*, 2009, 2011]. *Wang et al.* [2009], however, show that the early maximum in extreme wind speeds occurred during summer, whereas for winter upward trends in storminess can be found in the North Sea area. A recent extension of their study including western and central Europe confirms considerable seasonal differences of the calculated trends [*Wang et al.*, 2011].

[3] Available studies on past storm trends over the last century make use of pressure records, calculating geostrophic wind speeds from pressure differences or considering local pressure tendencies as a proxy for storm occurrences. They do not use wind speed measurements, as this quantity is easily affected by inhomogeneities, e.g., through changes in station surroundings, instruments and location. For the present study we make use of the newly available 20th Century Reanalysis [*Compo et al.*, 2011] covering the period from 1871 to 2008, which provides both pressure and simulated wind speed on the underlying model's grid. It is expected to be less affected by inhomogeneities for individual stations due to quality checks and the assimilation procedure, providing physically consistent fields. The results are validated against the well established but shorter NCEP and ERA40 reanalysis for the overlapping periods since about 1950, which have a considerably larger data basis for the assimilation. This study enhances previous assessments of long-term trends in storminess by analyzing trends in two different storminess measures (and considering different thresholds for each) in reanalysis data sets rather than analyzing station pressure records only. Note, however, that trends in reanalysis wind speeds may differ from observations [*Smits et al.*, 2005], partly explained by surface roughness changes affecting the recorded wind speeds [*Vautard et al.*, 2010].

2. Data and Methods

[4] The newly available Twentieth Century Reanalysis (20CR) covers the period 1871–2008. It assimilates surface pressure observations only [*Compo et al.*, 2006, 2011] into an atmospheric model on a horizontal resolution of T62 (approximately 1.9°) and also uses observed monthly sea-surface temperatures and sea-ice distributions as boundary conditions. An Ensemble Kalman Filter is used to optimally combine the imperfect observations and estimates of current state, producing an ensemble of 56 realizations of the reanalysis [*Compo et al.*, 2011]. This allows an investigation

[1]Climate Change Research Centre, University of New South Wales, Sydney, New South Wales, Australia.
[2]Institute of Meteorology, Freie Universität Berlin, Berlin, Germany.
[3]Swiss Reinsurance Company, Zurich, Switzerland.
[4]School of Geography, Earth and Environmental Sciences, University of Birmingham, Birmingham, UK.

0094-8276/11/2011GL047995

Table 1. Mean Annual Gale Day Frequencies and 95th Percentiles of Daily Maximum Wind Speeds During the Period 1960–2000 Are Shown for the Different Data Sets and Investigation Areas Used in This Study

Region	Abbreviation	Central Point of Investigation Area	Mean Annual Number of Gale Days G > 35 hPa (1960–2000)			Mean Annual 95th Percentile of Daily Max Wind Speeds (1960–2000), (ms^{-1})		
			20CR	NCEP1	ERA40	20CR	NCEP1	ERA40
North Sea North	NSN	60N, 5E	10.4	9.6	9.7	19.0	17.7	13.9
British Isles	BI	55N, 5W	19.6	19.6	21.6	19.1	15.8	11.3
North Sea Central	NSC	55N, 5E	10.7	11.3	13.4	17.3	16.1	13.0
Baltic Sea	BS	55N, 15E	6.0	7.2	9.7	14.0	12.4	9.4
Channel	CHA	50N, 0E	9.6	10.2	12.0	16.1	13.2	9.3
Central Europe	CE	50N, 10E	3.0	4.2	5.5	10.1	9.8	6.0

of the observational uncertainties in the data assimilation. Output data are provided on a regular 2° × 2° grid.

[5] Two state-of-the-art reanalyses, assimilating a considerably larger set of 3-dimensional atmospheric observations, are used to validate the 20CR results for the recent five to six decades: NCEP reanalysis [*Kistler et al.*, 2001] covering the years from 1948 to present and ERA40 [*Uppala et al.*, 2005] available for the period 1958 to 2001. ERA40 reanalysis data are available on a spatial resolution of about 1.125° (N80); the NCEP model also works on a T62 spectral grid, the reanalysis output of NCEP is provided on a 2.5° × 2.5° grid. For the calculation of the different measures of storminess, we make use of simulated daily mean-sea-level pressure (MSLP) and near-surface wind speeds, i.e., 10 m (ERA40) or the lowest model layer (NCEP, 20CR). The MSLP fields of all data sets are interpolated onto a uniform 2.5° × 2.5° regular grid prior to the calculation of geostrophic gale indices.

[6] Two measures of storminess, representing storm day frequency and local extreme wind speeds, are considered:

[7] 1. For quantifying storm day frequency, a gale index (known as "Jenkinson-Collinson" [*Jones et al.*, 1993]) is calculated using geostrophic approximation from the MSLP values at the grid points in a range of ±15 degrees around the central point of each investigation area. Terms for directional flow (F) and vorticity (Z) are derived from the spatial pressure differences and are subsequently used for calculating the gale index $G = \sqrt{\left(F^2 + \left(\frac{1}{2}Z\right)^2\right)}$. Details of the calculation of the geostrophic flow indices are given by *Jones et al.* [1993]. For this study we identify annual (seasonal) sums of gale days (G > 35 hPa) and severe gale days (G > 40 hPa) as measures of storm frequency. However, as the findings are generally similar for both, we restrict the presentation of results to the first threshold. Recent studies have shown this gale index to be well suited to the investigation of synoptic-scale storm situations in both reanalysis [*Donat et al.*, 2010a] and climate model data [*Donat et al.*, 2010b]. In this study we present the gale day frequencies calculated from large-scale geostrophic flow for six investigation areas in central, western and northern Europe (Table 1).

[8] 2. The 95th, 98th and 99th annual (seasonal) percentiles of daily maximum wind speeds are analyzed to represent the local intensity of extreme storm events and ensure comparability with previous studies [*Alexandersson et al.*, 1998, 2000; *Wang et al.*, 2009]. We find that results are generally similar across the different thresholds (though slightly more significant for the lower) and we therefore only show results derived for the 95th percentile of daily maximum wind speeds. Wind speed percentiles are calculated from the daily maxima of simulated wind speeds for 00, 06, 12 and 18 UTC at each grid box, and time series are presented for the same regions as the gale day frequencies (Table 1). For the time series (Figure 2), the field averages of wind speeds in the 3 × 3 grid boxes around the central point of the investigation area are considered. Trend calculations are, however, almost identical if only one grid box representative of the central point is used.

[9] Long-term trends are fitted with an ordinary least squares regression. For better comparison between the different investigation areas, the original time series are normalized prior to the trend fitting by removing the mean and dividing by the standard deviation, as by *Wang et al.* [2009]. The statistical significance of the trends is estimated using a Mann-Kendall-Test [*Kendall*, 1975]. Note that all evaluations cover the whole year unless otherwise specified.

3. Results

[10] In all three datasets, both the frequency of gale days and the magnitude of extreme wind speeds show a pronounced southeast-northwest gradient over Europe (Table 1). The annual mean number of gale days is highest over northwestern Europe and the North Sea region (BI, NSC, CHA, NSN), followed by Baltic Sea (BS) and Central Europe (CE). The spatial distribution of extreme wind speeds is generally similar; the simulated near-surface wind speeds are, however, subject to surface friction and thus stronger drag over land areas. Consequently the order is slightly modified when looking at absolute wind speeds, with slightly lower values over BI compared to NSN.

[11] For all sub-areas considered, time series of gale day frequencies and high wind percentiles are in good agreement between the different reanalysis datasets for their overlapping periods (Figure 1), with Spearman correlation coefficients generally above 0.7 (and a maximum of 0.98). On average, the correlation coefficients are higher for the MSLP-based storm frequency measure than for the high wind speed percentile. These comparisons confirm that the 20CR reproduces the occurrence of European wind storms well in spite of only assimilating surface pressure observations compared to the much more comprehensive set of 3-dimensional variables assimilated by the other reanalysis products. Note that this result may be related to the high observation density over the European continent and adjacent sea areas. We assume that 20CR should also provide

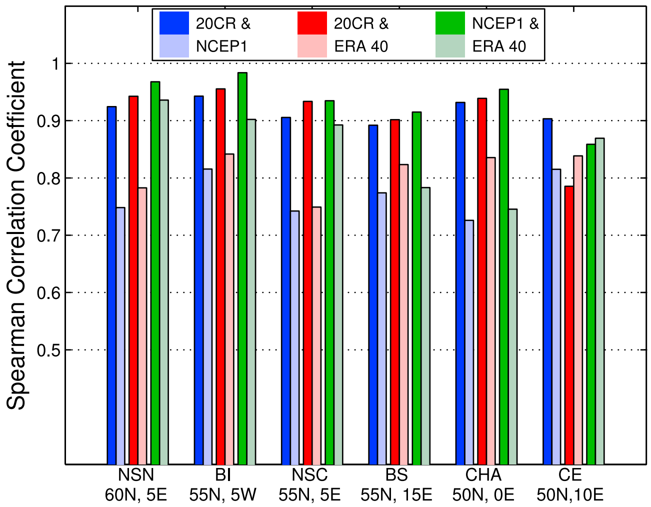

Figure 1. Spearman correlation coefficients of the storminess measures for each region between the different data sets. Correlations are calculated for the overlapping periods of the pairs of reanalysis data sets; 20CR and NCEP: 1948–2008 (blue); 20CR and ERA40: 1957–2002 (red); NCEP and ERA40: 1957–2002 (green). Each dark coloured (left) bar shows the correlation of annual frequency of gale days G > 35, the light coloured (right) bars are for the annual 95th percentile of daily maximum wind speeds. All correlations are significant at the 5% level.

reasonable estimates of storm activity back to 1871, given that Europe is relatively observation-rich throughout the whole period [*Compo et al.*, 2011]. X. L. Wang et al. (Extra-tropical cyclone activity in the ensemble of the Twentieth Century Reanalysis (20CRv2), 2010, available at http://www.joss.ucar.edu/events/2010/acre/agenda.html) found 20CR to be homogeneous during the past century in the areas of interest, whereas inhomogeneities are reported in data sparse regions. Considering the 56 ensemble members further allows estimation of observation-related uncertainties.

[12] Both storminess measures display pronounced variability on (multi-) decadal time scales. For most regions, phases of high storm activity are found during the first decades of the 20th century (Figure 2), although the specific magnitudes of the individual peaks differ for both storminess measures and in the different regions. A minimum in storm activity is generally found around 1960, followed by steep increase and a maximum storm activity during the 1990s, and a decline to average values in the first decade of the 21st century. Unprecedented high values of both storminess measures are found during the maximum in the late 20th century, around 1990, in the North Sea and Baltic Sea regions (BI, NSN, NSC, BS). Annual gale day frequencies are unprecedented in all regions during the latest maximum (Figure 2, left). Statistically significant positive trends over the whole 20C period are found for all investigation areas in central, western and northern Europe, with mean standardized trends ranging from 0.06 to 0.08 std/10 yr (gale days) and 0.04 to 0.10 std/10 yr (extreme wind speeds). This corresponds to absolute gale day frequency increases between 0.1/10 yr (CE) and 0.5/10 yr (BI) and respective for 95th percentile of wind speeds between 0.03 ms^{-1}/10 yr (CHA) and 0.09 ms^{-1}/10 yr (NSN). Trends tend to be even stronger for the most recent decades since about 1950, when a number of state-of-the-art reanalyses are available. Trends for winter (DJF) months only are similar on the whole (not shown), whereas slightly negative (and generally not significant) trends can be found for summer (JJA). We find enhanced extreme wind speeds during summer around 1920 in some regions (NSC, CH, CE), contributing to the early local maxima of the annual wind speed percentiles. Only occasional single occurrences of gale day events G > 35 hPa during summer are found throughout the investigation period. By far the majority of gale days and (synoptic-scale) high wind speeds occur during winter in Europe.

[13] The storm activity measures are calculated for all 56 ensemble members and allow an estimation of the effect of observational uncertainties on the storm trend calculations. The spread (grey areas in Figure 2) of the gale day frequencies and extreme wind speeds in the 56 realizations is generally larger towards the beginning of the analysis period, as expected given the potentially lower quality and smaller number of stations available for assimilation. Nevertheless, all realizations exhibit significant trends ($p \leq 0.08$ even for the weakest trend of extreme wind speeds in CHA).

[14] Over southern Europe and the Mediterranean region, the correlations of the storminess measures in the different data sets are generally lower (not shown), suggesting a lower confidence in 20CR for trend estimations in these areas. Examining the trends of 20CR extreme wind speeds at each grid point (Figure 3) confirms the picture gained from the time series at individual sub-regions. Significant increases in extreme wind speeds over the 138 yr period are found over north (Scandinavia), northwest (British Isles, North Sea) and central Europe, whereas trends in the remaining regions are mostly not significant. A small region around the Adriatic Sea exhibits negative trends.

4. Summary, Discussion and Conclusions

[15] Trends of European storminess are analyzed from three different reanalysis data sets, namely NCEP, ERA40 and 20CR. The newly available 20CR covers the past 138 years, back to 1871, allowing an examination of long-term trends beyond decadal-scale variability. Two different measures of storminess are examined, one quantifying the frequency of storm days, the other the magnitude of extreme wind speeds in relation to storm events. Intercomparison of

Figure 2. Time series of storm activity, (left) annual number of gale days and (right) annual 95th percentile of daily maximum wind speeds in the different regions based on the different reanalysis data sets. Solid lines show 11 yr running means of the normalized storminess measures in 20CR ensemble mean (blue), NCEP (green) and ERA40 (red), the grey shaded ranges indicate the spread between the maximum and minimum value of the 56 ensemble members of 20CR. Linear trends are indicated by the dashed lines, trend parameters slope (m, unit: standard deviations per 10 yr) and significance (p, Mann-Kendall-Test) are provided for each time series.

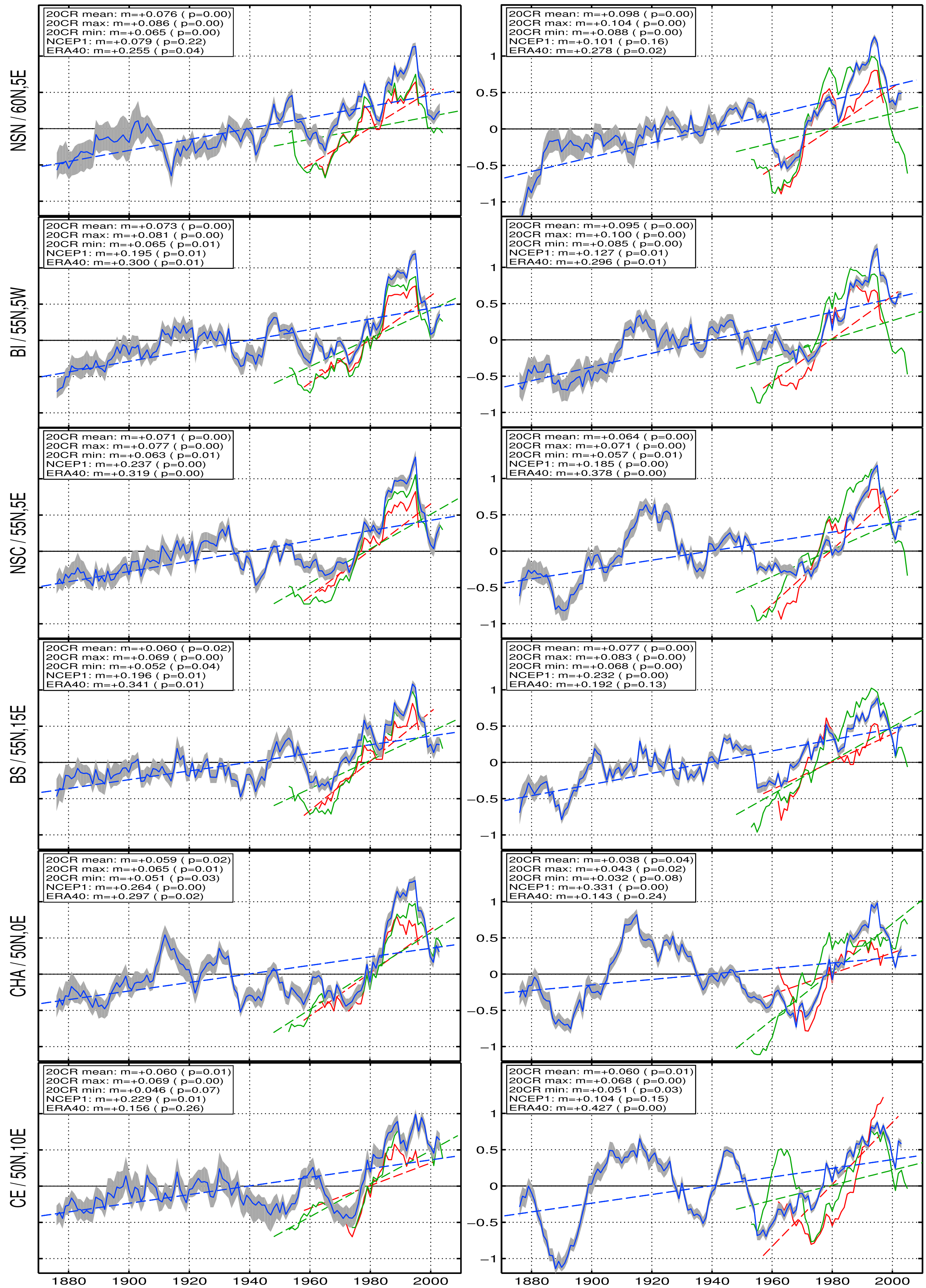
NSN / 60N,5E
BI / 55N,5W
NSC / 55N,5E
BS / 55N,15E
CHA / 50N,0E
CE / 50N,10E
20CR mean: m=+0.076 (p=0.00)
20CR max: m=+0.086 (p=0.00)
20CR min: m=+0.065 (p=0.00)
NCEP1: m=+0.079 (p=0.22)
ERA40: m=+0.255 (p=0.04)
20CR mean: m=+0.098 (p=0.00)
20CR max: m=+0.104 (p=0.00)
20CR min: m=+0.088 (p=0.00)
NCEP1: m=+0.101 (p=0.16)
ERA40: m=+0.278 (p=0.02)
20CR mean: m=+0.073 (p=0.00)
20CR max: m=+0.081 (p=0.00)
20CR min: m=+0.065 (p=0.01)
NCEP1: m=+0.195 (p=0.01)
ERA40: m=+0.300 (p=0.01)
20CR mean: m=+0.095 (p=0.00)
20CR max: m=+0.100 (p=0.00)
20CR min: m=+0.085 (p=0.00)
NCEP1: m=+0.127 (p=0.01)
ERA40: m=+0.296 (p=0.01)
20CR mean: m=+0.071 (p=0.00)
20CR max: m=+0.077 (p=0.00)
20CR min: m=+0.063 (p=0.01)
NCEP1: m=+0.237 (p=0.00)
ERA40: m=+0.319 (p=0.00)
20CR mean: m=+0.064 (p=0.00)
20CR max: m=+0.071 (p=0.00)
20CR min: m=+0.057 (p=0.01)
NCEP1: m=+0.185 (p=0.00)
ERA40: m=+0.378 (p=0.00)
20CR mean: m=+0.060 (p=0.02)
20CR max: m=+0.069 (p=0.00)
20CR min: m=+0.052 (p=0.04)
NCEP1: m=+0.196 (p=0.01)
ERA40: m=+0.341 (p=0.01)
20CR mean: m=+0.077 (p=0.00)
20CR max: m=+0.083 (p=0.00)
20CR min: m=+0.068 (p=0.00)
NCEP1: m=+0.232 (p=0.00)
ERA40: m=+0.192 (p=0.13)
20CR mean: m=+0.059 (p=0.02)
20CR max: m=+0.065 (p=0.01)
20CR min: m=+0.051 (p=0.03)
NCEP1: m=+0.264 (p=0.00)
ERA40: m=+0.297 (p=0.02)
20CR mean: m=+0.038 (p=0.04)
20CR max: m=+0.043 (p=0.02)
20CR min: m=+0.032 (p=0.08)
NCEP1: m=+0.331 (p=0.00)
ERA40: m=+0.143 (p=0.24)
20CR mean: m=+0.060 (p=0.01)
20CR max: m=+0.069 (p=0.00)
20CR min: m=+0.046 (p=0.07)
NCEP1: m=+0.229 (p=0.01)
ERA40: m=+0.156 (p=0.26)
20CR mean: m=+0.060 (p=0.01)
20CR max: m=+0.068 (p=0.00)
20CR min: m=+0.051 (p=0.03)
NCEP1: m=+0.104 (p=0.15)
ERA40: m=+0.427 (p=0.00)
1880 1900 1920 1940 1960 1980 2000
1 0.5 0 −0.5 −1

Figure 2

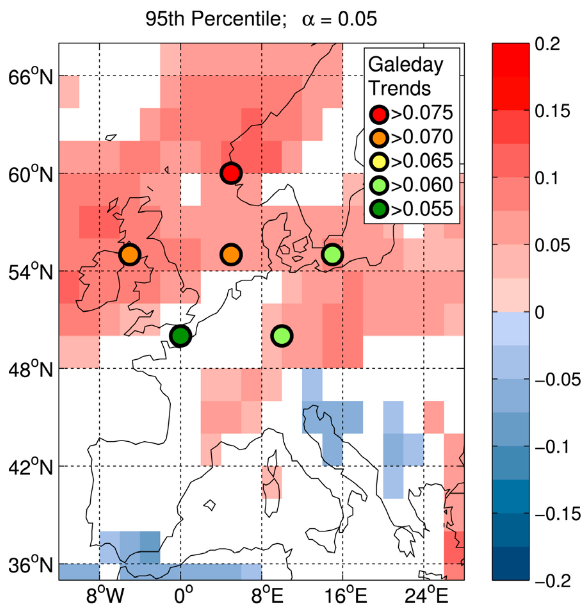

Figure 3. Trends in the annual 95th percentile of daily maximum wind speeds in 20CR ensemble mean during the period 1871–2008 (unit: std/10 yr). Trends are only plotted where significant ($p \leq 0.05$, Mann-Kendall-Test). The circles indicate the respective gale day trends at the specific locations from Figure 2.

the storminess measures calculated from the different data sets shows that 20CR, assimilating only surface pressure observations, is capable of reproducing the measures of storminess calculated from the NCEP and ERA40 reanalyses. Our results confirm previous studies in showing a high decadal-scale variability in the occurrence of wind storms in Europe [e.g., *Alexandersson et al.*, 2000; *Bärring and von Storch*, 2004; *Wang et al.*, 2009]. These previous works, using only station pressure records, identified periods of high storm activity during the late 19th / early 20th century, which was of similar magnitude to the recent maximum around 1990. In contrast, our results suggest that storminess was more intense during the recent maximum, in particular over the North Sea and Baltic Sea regions. We detect significant upward trends in both storminess measures since 1871 in many parts of western, central and northern Europe. It is not clear from this study what the causes of the identified trends are. On the one hand, climate model experiments often show more frequent and stronger wind storms in Europe under enhanced greenhouse gas forcing [e.g., *Leckebusch et al.*, 2006; *Pinto et al.*, 2007; *Donat et al.*, 2010b]. This suggests that the identified trends may (at least partly) be a consequence of increasing GHG concentrations during the past century although uncertainties remain in future projections [*Woollings*, 2010]. On the other hand, enhanced natural variability cannot be excluded from the recent maximum of storm activity.

[16] Some differences are apparent between storm trend estimations in reanalyses compared to station data. For wind speed measures, those differences [e.g., *Smits et al.*, 2005] may at least partly be explained by land use change, resulting in increased surface roughness, and leading to stilling of wind speeds [*Vautard et al.*, 2010]. However, studies using pressure-based proxies for storminess [e.g., *Hanna et al.*, 2008; *Wang et al.*, 2009] do not find as strong increases as we do and rather highlight the large decadal-scale variability of storminess. Nevertheless, *Wang et al.* [2011] report an unprecedented maximum in the early 1990s in the North Sea-British Isles area. Since the 20CR provides global physically consistent fields over 100+ years it is expected to be less affected by errors or inhomogeneities at individual stations. However, the 20CR is likely to suffer from some inhomogeneity due to the changing station density and the unknown quality of some early observations. Compared to other regions, the observation density is high in Europe throughout the investigation period [*Compo et al.*, 2011]. Observational uncertainty is further accounted for by considering the 56 ensemble realizations of the 20CR, all of them showing robust upward trends in the western, central and northern European investigation areas.

[17] Further in-depth analyses of 20CR are warranted, focusing on the variability and trends in atmospheric features related to storm events, such as storm tracks, extratropical cyclones, and teleconnection patterns. This may also help to understand the periods of high storm activity in the late 19th / early 20th century, partly occurring during summer months (compare to *Wang et al.* [2009]) and also to attribute mechanisms to explain the detected trends.

[18] **Acknowledgments.** Support for the Twentieth Century Reanalysis Project dataset is provided by the U.S. Department of Energy, Office of Science Innovative and Novel Computational Impact on Theory and Experiment (DOE INCITE) program, and Office of Biological and Environmental Research (BER), and by the National Oceanic and Atmospheric Administration Climate Program Office. We thank the European Centre for Medium-Range Weather Forecasts (ECMWF) and Deutscher Wetterdienst (DWD) for ERA40 reanalysis data availability. M.G. Donat and L.V. Alexander are supported by the Australian Research Council grants LP100200690 and CE110001028. We are also grateful to two anonymous reviewers for their helpful suggestions.

[19] The Editor thanks the two anonymous reviewers for their assistance in evaluating this paper.

References

Alexandersson, H., T. Schmith, K. Iden, and H. Tuomenvirta (1998), Long-term variations of the storm climate over NW Europe, *Global Atmos. Ocean Syst.*, *6*, 97–120.

Alexandersson, H., H. Tuomenvirta, T. Schmith, and K. Iden (2000), Trends of storms in NW Europe derived form an updated pressure data set, *Clim. Res.*, *14*, 71–73, doi:10.3354/cr014071.

Bärring, L., and H. von Storch (2004), Scandinavian storminess since about 1800, *Geophys. Res. Lett.*, *31*, L20202, doi:10.1029/2004GL020441.

Compo, G. P., J. S. Whitaker, and P. D. Sardeshmukh (2006), Feasibility of a 100 year reanalysis using only surface pressure data, *Bull. Am. Meteorol. Soc.*, *87*, 175–190, doi:10.1175/BAMS-87-2-175.

Compo, G. P., J. S. Whitaker, P. D. Sardeshmukh, N. Matsui, R. J. Allan, et al. (2011), The Twentieth Century Reanalysis project, *Q. J. R. Meteorol. Soc.*, *137*, 1–28, doi:10.1002/qj.776.

Donat, M. G., G. C. Leckebusch, J. G. Pinto, and U. Ulbrich (2010a), Examination of wind storms over central Europe with respect to circulation weather types and NAO phases, *Int. J. Climatol.*, *30*, 1289–1300, doi:10.1002/joc.1982.

Donat, M. G., G. C. Leckebusch, J. G. Pinto, and U. Ulbrich (2010b), European storminess and associated circulation weather types: Future changes deduced from a multi-model ensemble of GCM simulations, *Clim. Res.*, *42*, 27–43, doi:10.3354/cr00853.

Donat, M. G., G. C. Leckebusch, S. Wild, and U. Ulbrich (2011), Future changes in European winter storm losses and extreme wind speeds inferred from GCM and RCM multi-model simulations, *Nat. Hazards Earth Syst. Sci.*, *11*, 1351–1370, doi:10.5194/nhess-11-1351-2011.

Gastineau, G., and B. J. Soden (2009), Model projected changes of extreme wind events in response to global warming, *Geophys. Res. Lett.*, *36*, L10810, doi:10.1029/2009GL037500.

Hanna, E., J. Cappelen, R. Allan, T. Jónsson, F. le Blancq, T. Lillington, and K. Hickey (2008), New insights into north European and North Atlantic surface pressure variability, storminess and related climatic change since 1830, *J. Clim.*, *21*(24), 6739–6766, doi:10.1175/2008JCLI2296.1.

Jones, P. D., M. Hulme, and K. R. Briffa (1993), A comparison of Lamb circulation types with an objective classification scheme, *Int. J. Climatol.*, *13*, 655–663, doi:10.1002/joc.3370130606.

Kendall, M. G. (1975), *Rank Correlation Methods*, Charles Griffin, London.

Kistler, R., et al. (2001), The NCEP-NCAR 50-year reanalysis: Monthly means CD-ROM and documentation, *Bull. Am. Meteorol. Soc.*, *82*, 247–267, doi:10.1175/1520-0477(2001)082<0247:TNNYRM>2.3.CO;2.

Leckebusch, G. C., B. Koffi, U. Ulbrich, J. G. Pinto, T. Spangehl, and S. Zacharias (2006), Analysis of frequency and intensity of winter storm events in Europe on synoptic and regional scales from a multi-model perspective, *Clim. Res.*, *31*, 59–74, doi:10.3354/cr031059.

Meehl, G. A., et al. (2007), Global climate projections, in *Climate Change 2007: The Physical Science Basis. Contribution of Working Group I to the Fourth Assessment Report of the Intergovernmental Panel on Climate Change*, edited by S. Solomon et al., pp. 747–845, Cambridge Univ. Press, Cambridge, U. K.

Pinto, J. G., U. Ulbrich, G. C. Leckebusch, T. Spangehl, M. Reyers, and S. Zacharias (2007), Changes in storm track and cyclone activity in three SRES ensemble experiments with the ECHAM5/MPIOM1 GCM, *Clim. Dyn.*, *29*, 195–210, doi:10.1007/s00382-007-0230-4.

Smits, A., A. M. G. Klein Tank, and G. P. Koennen (2005), Trends in storminess over the Netherlands, 1962–2002, *Int. J. Climatol.*, *25*, 1331–1344, doi:10.1002/joc.1195.

Ulbrich, U., G. C. Leckebusch, and J. G. Pinto (2009), Cyclones in the present and future climate: A review, *Theor. Appl. Climatol.*, *96*, 117–131, doi:10.1007/s00704-008-0083-8.

Uppala, S. M., et al. (2005), The ERA-40 re-analysis, *Q. J. R. Meteorol. Soc.*, *131*, 2961–3012, doi:10.1256/qj.04.176.

Vautard, R., J. Cattiaux, P. Yiou, J. N. Thepaut, and P. Ciais (2010), Northern Hemisphere atmospheric stilling partly attributed to an increase in surface roughness, *Nat. Geosci.*, *3*, 756–761, doi:10.1038/ngeo979.

Wang, X. L., F. W. Zwiers, V. R. Swail, and Y. Feng (2009), Trends and variability of storminess in the northeast Atlantic region, 1874–2007, *Clim. Dyn.*, *33*, 1179–1195, doi:10.1007/s00382-008-0504-5.

Wang, X. L., H. Wan, F. W. Zwiers, V. R. Swail, G. P. Compo, R. J. Allan, R. S. Vose, S. Jourdain, and X. Yin (2011), Trends and low-frequency variability of storminess over western Europe, 1878–2007, *Clim. Dyn.*, doi:10.1007/s00382-011-1107-0, in press.

Woollings, T. (2010), Dynamical influences on European climate: An uncertain future, *Philos. Trans. R. Soc A*, *368*, 3733–3756, doi:10.1098/rsta.2010.0040.

L. V. Alexander and M. G. Donat, Climate Change Research Centre, University of New South Wales, Sydney, NSW 2052, Australia. (m.donat@unsw.edu.au)

G. C. Leckebusch, D. Renggli, U. Ulbrich, and S. Wild, Institute of Meteorology, Freie Universität Berlin, Carl-Heinrich-Becker-Weg 6-10, D-12165 Berlin, Germany.